

Influence of internal energy and impact angle on the sticking behaviour of reactive radicals in thin a-C:H film growth: a molecular dynamics study

E. Neyts and A. Bogaerts

Received 14th December 2005, Accepted 8th March 2006

First published as an Advance Article on the web 20th March 2006

DOI: 10.1039/b517563a

In this molecular dynamics study, we investigate the influence of the internal energy and the impact angle on the sticking coefficients of several hydrocarbon radicals on a hydrogenated amorphous carbon surface. The selected radical species and their kinetic energy were determined experimentally. However, no information is available regarding their internal energy, nor on their impact angles. It is shown that the internal energy has a considerable influence on the sticking coefficient, which is dependent on the kind of species. The impact angle, however, is shown to be of minor importance.

Introduction

In the last decade, amorphous carbons and hydrogenated amorphous carbons have become technologically important materials in a wide range of applications.¹ Examples include their use as protective coatings, *e.g.* on computer hard discs, as solid lubricants, as biocompatible coatings or in electronic devices.^{2,3} Their widespread use is due to their attractive tribological, mechanical and optical properties. These properties are determined by the microstructure of the film, which is in turn determined by the deposition technique used for its fabrication. Often, the different types of amorphous carbon materials are characterised by their $sp^2 : sp^3$ ratio, their hydrogen content, and some specific properties, such as hardness, density or refractive index. Essentially, the resulting film exhibits these properties due to the actual growth mechanism that produces the film. Therefore, a parameter study investigating the numerous factors governing the deposition mechanism enables us to optimize the growth of films in terms of their properties. In the present work, the influence of the internal energy and impact angle of the bombarding species on their reaction probability (more specifically, their sticking coefficients) are investigated, because these parameters are often not exactly known from experiment. Sticking coefficients are also important parameters both in plasma simulations and in real plasmas.⁴

Previously, we have already simulated the current model system,^{5–8} focusing on the actual deposition of thin a-C:H layers, as well as on the reaction mechanisms of various hydrocarbon radicals, but we have not yet investigated their reaction mechanisms as a function of their internal energy or impact angle.

Other groups have also used molecular dynamics (MD) simulations to study the deposition, structure, relaxation and properties of a-C(:H) and ta-C(:H) films. Belov,⁹ Jäger and

Albe¹⁰ and Belov and Jäger^{11–16} have investigated the structure, relaxation and properties of ta-Cs using MD simulations employing both the Tersoff¹⁷ and Brenner^{18,19} potentials. They also investigated the growth of ta-C films using MD simulations, bombarding the substrate with medium energy C atoms and C₂H₂ molecules (*ca.* ~100 eV), using the same methodology as applied in our work.

Similar growth simulations were performed by Kaukonen and Nieminen.^{20,21} These simulations substantiate the validity of the subplantation mechanism for ta-C growth, showing how C atoms with energies of 40 eV and above become subplanted and coincidentally cause densification of the layer. These simulations show subplantation occurring starting at a C-impact energy of about 40 eV, and increasing with increasing energy.

On the other hand, recent simulations by Marks *et al.*^{22–24} illustrate that the growth of ta-C films is possible well below the subplantation threshold (*i.e.*, at an energy as low as 6 eV) using the environment-dependent interaction potential (EDIP).²⁵

Growth of thin hydrocarbon films from adamantane beams with hyperthermal energies (> 1 eV) was studied by Plaisted and Sinnott.²⁶

Hyperthermal atom and cluster beam growth (1–100 eV) of thin a-C(:H) films was further simulated by Zoppi *et al.*,²⁷ Plaisted *et al.*²⁸ and Halac *et al.*²⁹

MD simulations are also used to perform structural analyses of amorphous carbons, *e.g.* Gao *et al.*³⁰ investigated the effects of the structure of a-C:H films on the mechanical and tribological properties using the Brenner potential; Lee *et al.*³¹ studied the structural properties of a-C films as a function of the depositing atom beam energy using the Tersoff potential. Sinnott *et al.*³² employed MD simulations using the Brenner potential to study nanometer-scale indentation of amorphous carbons. Using the EDIP potential, Pearce *et al.*³³ investigated the thermal spike behaviour upon impact of medium high energy atoms (50–400 eV). The friction behaviour of a-C:H thin films was investigated by Zhang *et al.*³⁴ The evolution of

University of Antwerp, Department of Chemistry, Research group PLASMANT, Universiteitsplein 1, 2610 Antwerp, Belgium

sp^2 networks in a-C:H films with substrate temperature was studied by Gago *et al.*³⁵

On a more fundamental level, reaction mechanisms have been studied by several authors. Garrison *et al.*³⁶ demonstrated dimer opening by CH_x species ($x < 3$) on diamond {001} (2×1) surfaces using the Brenner potential.

Detailed reaction mechanisms of CH_3 radicals on diamond {111} surfaces have been investigated by Träskelin *et al.*³⁷ with both classical MD simulations using the Brenner potential and tight-binding (TB) simulations.

Finally, Perry and Raff^{38,39} studied the reaction mechanisms of several hydrocarbon radicals (*i.e.*, C_2H_2 , C_2H , CH_3 , CH_2 , C_2H_4 , C_2H_3 , C_3H and C_n ($n = 1-3$)) on a diamond {111} surface, also using the Brenner potential.

These simulations, however, are not immediately relevant for this work, since they focus mainly on atom and molecule impacts with kinetic energies above 1 eV and the formation of ta-C(:H) films. Furthermore, it should be realised that these simulations are not concerned with the reactive hydrocarbon radical reaction mechanisms on a-C:H surfaces, which are investigated in this work. Also, the influence of the internal energy and impact angle have not been investigated previously for the current model system.

However, the effect of the impact angle has already been studied for other systems. For instance, MD simulations of Cu impacts demonstrated the strong dependence of the sticking behaviour on the impact angle, showing how the sticking coefficient lowers drastically and leads to greater scattering as the impact angle increases.⁴⁰⁻⁴²

Surface loss probabilities of small C_xH_y hydrocarbon radicals on a-C:H films were determined experimentally by Hopf *et al.*,^{43,44} von Keudell *et al.*,⁴⁵ Perrin *et al.*⁴⁶ and Shiratani *et al.*⁴⁷ Temperature-dependent sticking coefficients of CH_3 radicals on a-C:H surfaces were determined experimentally by Meier and von Keudell.⁴⁸

To the knowledge of the authors, however, no data exist on the sticking behaviour of the hydrocarbon radicals as a function of their internal energy and impact angle as investigated in this work.

An efficient remote plasma source to deposit high-quality a-C:H films at a high deposition rate is the so-called expanding thermal plasma.^{49,50} The simulations presented in this work are based on the experimental deposition of a-C:H films using this source. However, the results are relevant for all deposition techniques where growth proceeds through hydrocarbon radical growth without ion bombardement, as in *e.g.* remote plasma sources without substrate bias or in sputter deposition.

Description of the simulation model

The MD code used in this work was originally developed by Serikov *et al.*⁵¹ and subsequently modified. In a MD simulation, the atoms in the system are followed through space and time, integrating their equations of motion. The integrator used is the velocity Verlet algorithm.⁵² The interatomic potential used in this work is the well-known original Brenner potential for hydrocarbons.¹⁸

Periodic boundary conditions are applied in the plane of the surface, *i.e.*, in the $\pm x$ and $\pm y$ directions. In Fig. 1, the

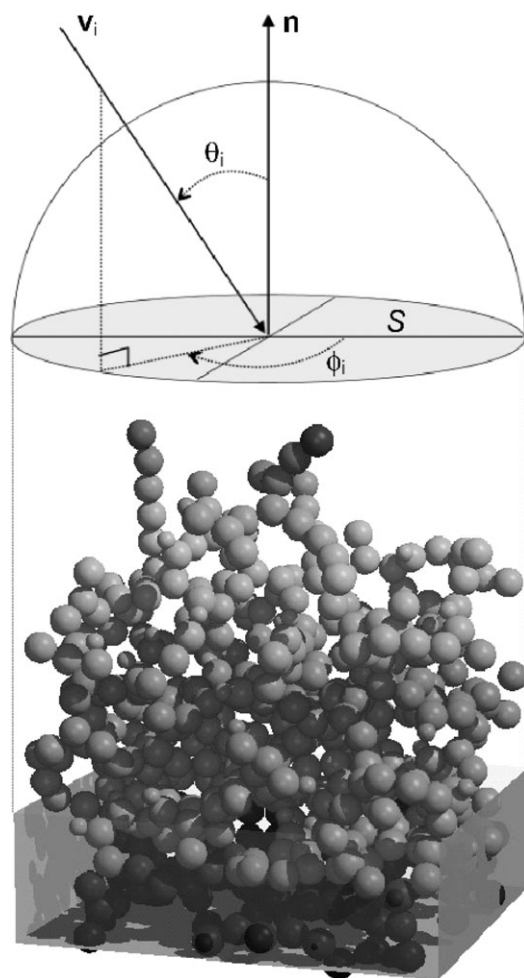


Fig. 1 Input substrate and definition of the polar impact angle θ_i and azimuthal angle ϕ_i . The vertical grey planes represent the periodic boundaries. The dark atoms at the bottom of the substrate are rigid.

periodic boundaries are the vertical grey planes. The bottom layers of the substrate were kept fixed to anchor the simulation cell. These bottom layers consisted of 128 atoms, corresponding to about the lower 20% of the substrate.

The substrate on which the radical impacts were performed was a previously simulated thin a-C:H film, containing 610 atoms. The atomic concentration of H in the film is calculated to be 9.5%, accommodated in the film by CH fragments, both in the bulk of the film and at the surface. Note that CH_2 fragments and CH_3 fragments are virtually non-existent in the film. This substrate was created by sequential radical impacts on a clean diamond {111} surface until a thickness of 10 nm was reached. To simulate the dissipation of heat out of the simulation cell after each radical impact, the Berendsen heat bath was used, including all non-fixed atoms, and set at 100.0 K using a rise time of 0.1 ps.⁵³ After the formation of the final structure (*i.e.*, after a thickness of 10 nm was reached), the diamond layer was removed, and the resulting structure was thermalized at 100.0 K, again using the Berendsen heat bath including all non-fixed atoms. After this thermalization stage, the substrate was allowed to relax. A more detailed discussion regarding the creation of the substrate is given in ref. 54.

The selected species are CH, C₂, C₂H, linear C₃ (l-C₃), linear C₃H (l-C₃H), cyclic C₃ (c-C₃) and cyclic C₃H (c-C₃H). The kinetic energy of the species was set to 0.13 eV, corresponding to the experimentally measured gas temperature of about 1500 K. No experimental information was available regarding the internal energy of the radicals. Therefore, we have chosen values over two orders of magnitude. The internal energy for each of the species was taken as {0.026; 0.50; 1.0; 2.0; 2.6 eV}. The selected polar impact angles were $\theta_i = \{0; 15; 30; 45^\circ\}$, while the azimuthal angle ϕ_i was chosen randomly. The impact angle θ_i is defined as the angle between the center-of-mass velocity vector v_i of the impinging radical and the normal n to the surface S , as shown in Fig. 1. The azimuthal angle ϕ_i is defined as the angle between the positive x -axis and the projection of v_i on the (x,y) plane, as also shown in Fig. 1. An integration time of 2 ps was chosen for the simulations using impact angles of 0 and 15°, while integration times of 2.2 and 2.4 ps were chosen for (polar) impact angles of 30 and 45°, respectively, to account for the longer path they travel before reaching the surface. The internal energy of the particles in the simulations using different impact angles was 0.026 eV.

Each calculation of the sticking coefficient for a species with a given impact angle and internal energy involved 500 impacts. As an example, the accumulated calculated sticking coefficients for the C₃H radical at an impact angle of 0° and different internal energies are shown in Fig. 2 as a function of the impact number. The plotted sticking coefficient s_i in this figure, at any impact number i , is given by:

$$s_i = \frac{\sum_{j=1}^i \delta_j}{i}$$

where δ_j is the Kronecker delta. A particle is considered to stick if at least one of its constituent atoms is bound to the surface. It can be seen in the figure that after 500 impacts, the sticking coefficient has converged to its final value. Also shown in Fig. 2 is the procentual difference between the calculated sticking coefficient at impact i and the so-called final calculated value (*i.e.*, after 500 impacts). The dashed horizontal lines indicate the $\pm 5\%$ boundaries, relative to the final value. The full horizontal lines indicate the $\pm 2\%$ boundaries. After about 200 impacts, the accumulated sticking coefficient has converged to within $\pm 5\%$ of its final value. This value converges to within 2% after about 400 impacts. Similar results (but typically showing somewhat faster convergence) were obtained for the other species.

Results and discussion

Effect of the internal energy

In Fig. 3, the calculated sticking coefficients for the different species are shown as a function of their internal energies. It can be seen that CH, C₂H and c-C₃H show a decrease in their sticking coefficient for increasing internal energies. On the other hand, the sticking coefficients of the l-C₃, l-C₃H and c-C₃ species show a slight increase as a function of their internal energy. Finally, the sticking coefficient of C₂ is nearly

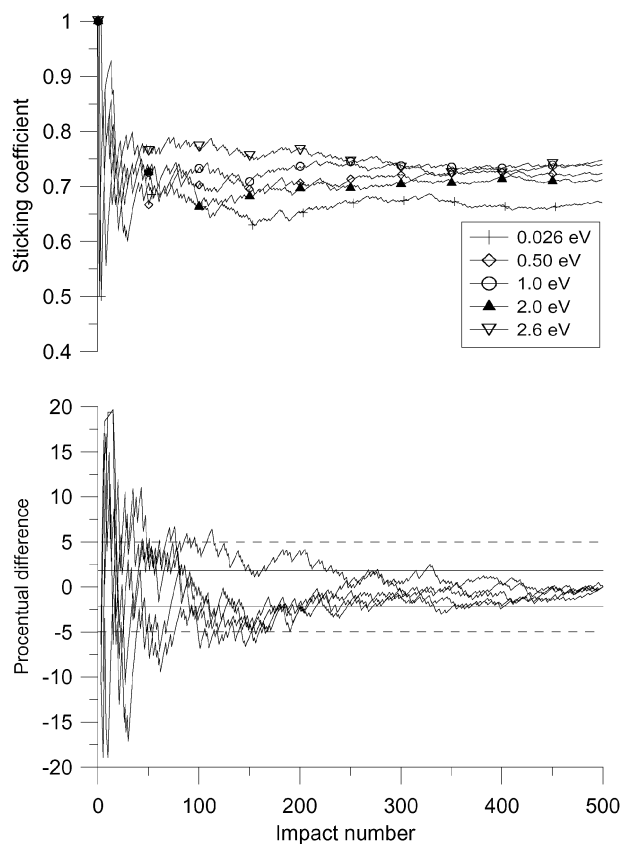


Fig. 2 Calculated accumulated sticking coefficients for the C₃H radical at an impact angle of 0° for different internal energies (top). Also shown is the procentual difference between the running accumulated sticking coefficient and the final value after 500 impacts (bottom). The dashed horizontal lines denote the $\pm 5\%$ boundaries, and the full horizontal lines the $\pm 2\%$ boundaries. The final sticking coefficients for the different energies are given in Fig. 2.

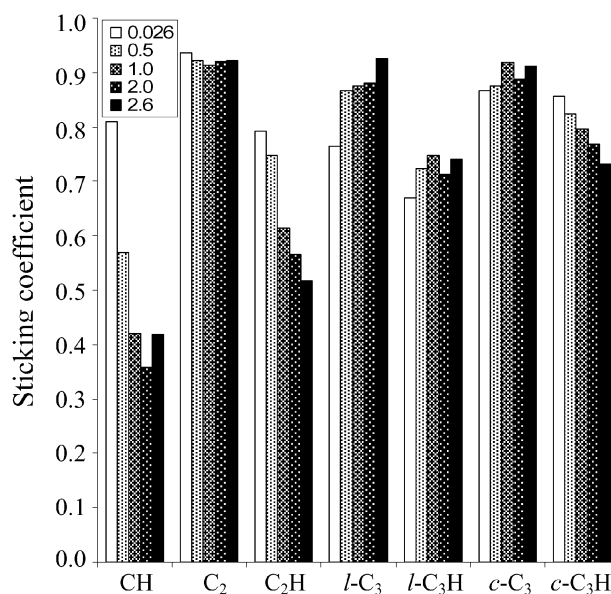


Fig. 3 Calculated sticking coefficients of the different species as a function of their internal energy, distributed among vibrational and rotational motion.

independent of its internal energy. In general, all species show a high sticking coefficient, varying between 0.4–0.9, due to their strong radical nature.

The species showing the highest sticking coefficient throughout the simulations is C_2 , with a sticking coefficient of above 0.9. Indeed, both of the C atoms have an unpaired electron, ready to pair with a radical site at the surface. Also, both C atoms are ‘free’, *i.e.*, unhindered and unshielded by a H atom. Therefore, the exact rotational orientation of the species relative to the surface is unimportant: at least one of the two C atoms is entirely free to react with the surface atoms, independent of its exact orientation towards the surface upon impact. Also, the vibrational part of the internal energy does not alter the sticking coefficient significantly, since only stretch vibrations are possible. This vibration mode does not affect the constituent atoms reaction probabilities.

The relevance of these effects becomes clear by comparison with C_2H . The sticking coefficient of C_2H is considerably lower than the C_2 sticking coefficient, and it is also much more dependent on the internal energy, varying from nearly 0.8 till about 0.5, for an internal energy between 0.026 and 2.6 eV, respectively. Indeed, while in C_2 , both C atoms can react with the surface, the C_2H radical will stick to the surface virtually always with the C atom that is not carrying the H atom. The other C atom is shielded by the H atom. Hence, in this case the orientation of the radical relative to the surface is limiting its reaction probability. Increasing the internal energy, and hence introducing more ‘violent’ vibrations, results in a decrease in the sticking coefficient. Indeed, since the H atom is very light, it moves much faster than the C atoms. Increasing the internal energy allows the H atom to cover a wider area around the C atom it is attached to. When the radical now approaches the surface, the repulsive forces between the radical and the surface atoms will become more apparent, due to the wider action radius of the H atom. In other words, the H atom that partially shields the radical from the surface widens its repulsive interaction range with the surface due to its amplified motion resulting from the increase in internal energy.

The same effect also occurs for CH, which shows a very similar trend in its sticking coefficient behaviour as a function of its internal energy, varying from 0.8 at 0.026 eV to about 0.35 at 2.0 eV. The slight increase for the highest internal energy chosen in this work, *i.e.*, 2.6 eV, is due to the strong increase in the fraction of impacts in which the radical breaks up upon impact and subsequently reacts with the surface, as shown in Fig. 4 (see below).

The $l-C_3$ radical is similar to C_2 in the sense that it has 2 C atoms which can freely react with the surface. The middle C atom, which is fully bound, almost never reacts with the surface.⁵⁵ Hence, the reaction probability of C_3 is nearly independent of its rotational orientation relative to the surface, similar to C_2 . In contrast to C_2 , however, the sticking coefficient of $l-C_3$ shows an additional dependence on its internal energy. A higher internal energy increases the number of sticking events with one of the outer C atoms, due to the lower influence of the middle C atom: as the molecule vibrates more, the radical is more non-linear, decreasing the repulsive interactions from the middle C atom with the surface.

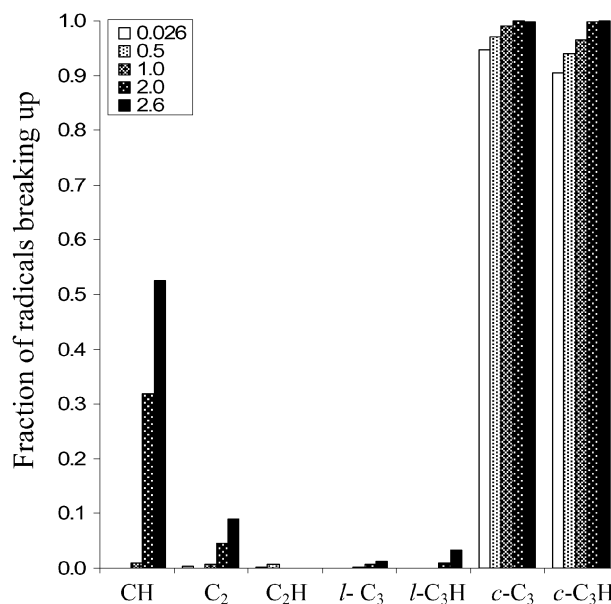


Fig. 4 Calculated fraction of sticking radicals that break up upon impact.

The same is true for the $l-C_3H$ radical, although here the effect is reduced by the effect of the increased H-interaction. Overall, the H atom is responsible for the lower sticking coefficient of $l-C_3H$ as compared to $l-C_3$.

The $c-C_3$ and $c-C_3H$ radicals are species with weak interatomic bonds, due to their structure: indeed, the 3-atom ring configuration introduces a ring stress lowering the interatomic bond strengths. Upon impact, most of these radicals break up, as shown in Fig. 4. Here, the fraction of the radicals that break up upon impact and subsequently stick on the surface is depicted. In this process, the radicals are converted into their respective linear counterparts. The calculated sticking coefficients for these species having high internal energies therefore correspond very closely to the values obtained for the linear species.

At lower internal energies, the calculated sticking coefficients are higher for the cyclic isomers compared to the linear isomers. This is caused by the reactivity of the unpaired electrons in the cyclic radicals, and the absence of a fully bound central atom in the cyclic isomers. Therefore, the radicals can easily react with the surface, leading to a high sticking coefficient. As the internal energy increases, more radicals are converted into their linear counterparts (due to the increase in the break-up events), and a fully bound central C atom is created, altering the sticking coefficient, such that it converges towards the value for the corresponding linear radical.

Effect of the impact angle

At medium hyperthermal impact energies (10–100 eV), the sticking behaviour of impacting particles is strongly dependent on the impact angle, drastically lowering the sticking coefficient and leading to greater scattering as the impact angle increases, as demonstrated in *e.g.* ref. 40–42 Here, we have also investigated the effect of the impact angle in the range between

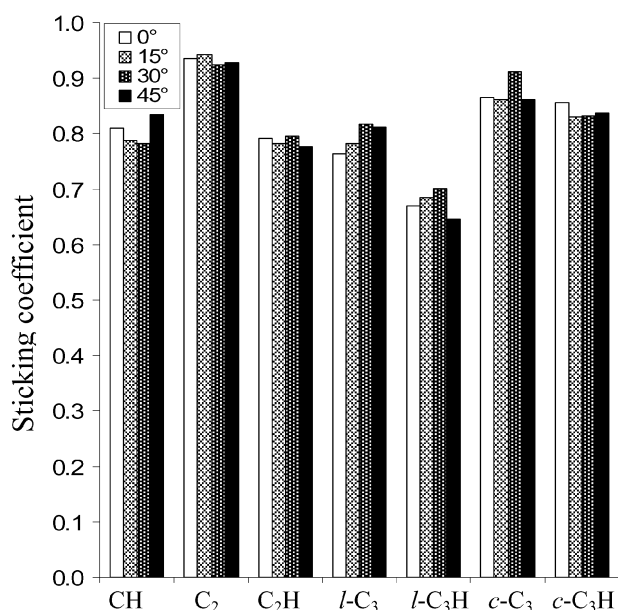


Fig. 5 Calculated sticking coefficients of the different species as a function of their impact angle.

0–45° on the sticking coefficients of the different radicals. Recall, however, that the incident energy of the radicals is only 0.13 eV. The results are shown in Fig. 5. It appears that the effect is minimal for all species. Furthermore, the reaction mechanisms for the different species remain unaltered when changing the impact angle. Hence, the effects described above remain valid under these circumstances. Possibly, this is due to the low kinetic energy of the species. Indeed, at low impact energies, the incoming radical has enough time to interact with the surface, irrespective of the impact angle, since the interaction time between the radical and the surface hardly changes with the impact angle. Hence, it appears that the assumption of normal incidence in MD simulations of bombarding species with low incident energies can give a realistic picture, even if the exact impact angle is not known.

Conclusion

MD simulations have been performed to investigate the effect of the internal energy of a set of hydrocarbon radicals on their sticking coefficients on a typical a-C:H surface. Additionally, the effect of the polar impact angle of the radicals was determined. The species and their translational energies were determined from an expanding thermal plasma experiment. It is found that the impact angle has no visible effect on the resulting sticking coefficients. The internal energy, on the other hand, has a pronounced effect on the calculated sticking coefficients. The effect is species dependent: while the sticking coefficient increases with rising internal energy for the linear C₃, linear C₃H and cyclic C₃ species, it decreases strongly for CH, C₂H and cyclic C₃H. The sticking coefficient of C₂ shows no dependence on the internal energy. The results are explained in terms of the species structure, composition and reaction mechanism. These results are relevant for a-C:H film deposition techniques where growth proceeds through radical

chemisorption, as in *e.g.* remote plasma sources. Furthermore, the sticking coefficients obtained can be used as input parameters in *e.g.* plasma simulations. Finally, the results show that the reliability of MD simulations of thin film growth using low kinetic energy species can be improved if experimental knowledge of the internal energies of the species is available.

Acknowledgements

E. Neyts is indebted to the Institute for the Promotion of Innovation by Science and Technology in Flanders (IWT-Flanders) for financial support. The authors would like to thank J. Benedikt and Prof. R. van de Sanden for the many fruitful discussions on the chemistry in the ETP plasma and the deposition mechanisms, and also Prof. R. Gijbels for the interesting discussions and for making this PhD work possible.

References

- 1 J. Robertson, *J. Non-Cryst. Solids*, 2002, **299–302**, 798.
- 2 J. Robertson, *Mater. Sci. Eng.*, 2002, **R37**, 129.
- 3 W. I. Milne, *Semicond. Sci. Technol.*, 2003, **18**, S81.
- 4 D.-S. Tsai, T.-C. Chang, W.-C. Hsin, H. Hamamura and Y. Shimogaki, *Thin Solid Films*, 2002, **411**, 177.
- 5 E. Neyts, A. Bogaerts, R. Gijbels, J. Benedikt and M. C. M. van de Sanden, *Nucl. Instrum. Methods B*, 2005, **228**, 315.
- 6 E. Neyts, A. Bogaerts, R. Gijbels, J. Benedikt and M. C. M. van de Sanden, *Diamond Relat. Mater.*, 2004, **13**, 1873.
- 7 E. Neyts, A. Bogaerts and M. C. M. van de Sanden, *J. Appl. Phys.*, 2006, **99**, 014902.
- 8 E. Neyts, A. Bogaerts and M. C. M. van de Sanden, *Diamond Relat. Mater.* DOI: 10.1016/j.diamond.2006.02.003.
- 9 A. Yu Belov, *Comput. Mater. Sci.*, 2003, **27**, 30.
- 10 H. U. Jäger and K. Albe, *J. Appl. Phys.*, 2000, **88**, 1129.
- 11 A. Yu Belov and H. U. Jäger, *Diamond Relat. Mater.*, 2005, **14**, 1014.
- 12 A. Yu Belov and H. U. Jäger, *Thin Solid Films*, 2005, **482**, 74.
- 13 A. Yu Belov and H. U. Jäger, *Comput. Mater. Sci.*, 2003, **27**, 16.
- 14 H. U. Jäger and A. Yu Belov, *Phys. Rev. B*, 2003, **68**, 024201.
- 15 A. Yu Belov and H. U. Jäger, *Mater. Res. Soc. Symp. Proc.*, 2001, **648**, 6.53.1.
- 16 H. U. Jäger and D. Weiler, *Diamond Relat. Mater.*, 1998, **7**, 858.
- 17 J. Tersoff, *Phys. Rev. Lett.*, 1988, **61**, 2879.
- 18 D. W. Brenner, *Phys. Rev. B*, 1990, **42**, 9458.
- 19 D. W. Brenner, O. A. Shenderova, J. A. Harrison, S. J. Stuart, B. Ni and S. B. Sinnott, *J. Phys.: Condens. Matter*, 2002, **14**, 783.
- 20 H. P. Kaukonen and R. M. Nieminen, *Phys. Rev. Lett.*, 1992, **68**, 620.
- 21 H. P. Kaukonen and R. M. Nieminen, *Phys. Rev. B*, 2000, **61**, 2806.
- 22 N. A. Marks, J. M. Bell, G. K. Pearce, D. R. McKenzie and M. M. Bilek, *Diamond Relat. Mater.*, 2003, **12**, 2003.
- 23 N. A. Marks, *Diamond Relat. Mater.*, 2005, **14**, 1223.
- 24 N. A. Marks, *J. Phys.: Condens. Matter*, 2002, **14**, 2901.
- 25 N. A. Marks, *Phys. Rev. B*, 2000, **63**, 035401.
- 26 T. A. Plaisted and S. B. Sinnott, *J. Vac. Sci. Technol., A*, 2001, **19**, 262.
- 27 L. Zoppi, L. Colombo and D. Donadio, *Eur. Phys. J. B*, 2002, **27**, 335.
- 28 T. A. Plaisted, B. Ni, J. D. Zahrt and S. B. Sinnott, *Thin Solid Films*, 2001, **381**, 73.
- 29 E. B. Halac, M. Reinoso, A. G. Dall'Asen and E. Burgos, *Phys. Rev. B*, 2005, **71**, 115431.
- 30 G. T. Gao, P. T. Mikulski, G. M. Chateaufneuf and J. A. Harrison, *J. Phys. Chem. B*, 2003, **107**, 11082.
- 31 S.-H. Lee, C.-S. Lee, S.-C. Lee and K.-R. Lee, *Surf. Coat. Technol.*, 2004, **177–178**, 812.
- 32 S. B. Sinnott, R. J. Colton, C. T. White, O. A. Shenderova, D. W. Brenner and J. A. Harrison, *J. Vac. Sci. Technol., A*, 1997, **15**, 936.

-
- 33 G. K. Pearce, N. A. Marks, D. R. McKenzie and M. M. M. Bilek, *Diamond Relat. Mater.*, 2005, **14**, 921.
- 34 S. Zhang, G. Wagner, S. N. Medyanik, W.-K. Liu, Y.-H. Yu and Y.-W. Chung, *Surf. Coat. Technol.*, 2004, **177–178**, 818.
- 35 R. Gago, M. Vinnichenko, H. U. Jäger, A. Yu Belov, I. Jimenez, N. Huang, H. Sun and M. F. Maitz, *Phys. Rev. B*, 2005, **72**, 014120.
- 36 B. J. Garrison, E. J. Dawnkaski, D. Srivastava and D. W. Brenner, *Science*, 1992, **255**, 835.
- 37 P. Träskelin, E. Salonen, K. Nordlund, A. V. Kraheninnikov and C. H. Wu, *J. Appl. Phys.*, 2003, **93**, 1826.
- 38 M. D. Perry and L. M. Raff, *J. Phys. Chem.*, 1994, **98**, 4375.
- 39 M. D. Perry and L. M. Raff, *J. Phys. Chem.*, 1994, **98**, 8128.
- 40 X.-Y. Liu, M. S. Daw, J. D. Kress, D. E. Hanson, V. Arunachalam, D. G. Coronell, C.-L. Liu and A. F. Voter, *Thin Solid Films*, 2002, **422**, 141.
- 41 C. F. Abrams and D. B. Graves, *IEEE Trans. Plasma Sci.*, 1999, **27**, 1426.
- 42 C. F. Abrams and D. B. Graves, *J. Appl. Phys.*, 1999, **86**, 2263.
- 43 C. Hopf, T. Schwarz-Selinger, W. Jacob and A. von Keudell, *J. Appl. Phys.*, 2000, **87**, 2719.
- 44 C. Hopf, K. Letourneur, W. Jacob, T. Schwarz-Selinger and A. von Keudell, *Appl. Phys. Lett.*, 1999, **74**, 3800.
- 45 A. von Keudell, C. Hopf, T. Schwarz-Selinger and W. Jacob, *Nucl. Fusion*, 1999, **39**, 1451.
- 46 J. Perrin, M. Shiratani, P. Kae-Nune, H. Videlot, J. Jolly and J. Guillon, *J. Vac. Sci. Technol., A*, 1998, **16**, 278.
- 47 M. Shiratani, J. Jolly, H. Videlot and J. Perrin, *Jpn. J. Appl. Phys.*, 1997, **36**, 4752.
- 48 M. Meier and A. von Keudell, *J. Chem. Phys.*, 2002, **116**, 5125.
- 49 J. W. A. M. Gielen, P. R. M. Kleuskens, M. C. M. van de Sanden, L. J. van IJzendoorn, D. C. Schram, E. H. A. Dekempeneer and J. Meneve, *J. Appl. Phys.*, 1996, **80**, 5986.
- 50 J. Benedikt, D. J. Eijkman, W. Vandamme, S. Agarwal and M. C. M. van de Sanden, *Chem. Phys. Lett.*, 2005, **402**, 37.
- 51 V. V. Serikov, S. Kawamoto, C. F. Abrams and D. B. Graves, *APS Proceedings of the 22nd Symposium on Rarefied Gas Dynamics*, Sydney, 2000.
- 52 W. C. Swope, H. C. Anderson, P. H. Berens and K. R. Wilson, *J. Chem. Phys.*, 1982, **76**, 637.
- 53 H. J. C. Berendsen, J. P. M. Postma, W. F. van Gunsteren, A. DiNola and J. R. Haak, *J. Chem. Phys.*, 1984, **76**, 3684.
- 54 E. Neyts, A. Bogaerts and M. C. M. van de Sanden, *Appl. Phys. Lett.*, in press.
- 55 D. N. Ruzic and D. A. Alman, presentation at the 10th International Workshop on Carbon Materials for Fusion Application, Jülich, 2003.